 doi:10.20944/preprints202011.0240.v1

Post-Mortem Cardiac Magnetic Resonance for the diagnosis of Hypertrophic Cardiomyopathy

Giovanni Donato Aquaro, MD[1], Benedetta Guidi, MD PhD[2], Federico Biondi, MD, Enrica Chiti, BSc[4], Alessandro Santurro, MD[5], Matteo Scopetti, MD[5], Emanuela Turillazzi, MD, PhD [2], Marco Di Paolo, MD[2].

[1]Fondazione Toscana G. Monasterio, Pisa, Italy

[2]UO Medicina legale, University of Pisa, Italy

[3]University of Trieste, Trieste, Italy

[4]Clinical and Translational Science Research Department, University of Pisa, Italy

[5] Department of Anatomical, Histological, Forensic and Orthopaedic Sciences, Sapienza University of Rome

Short title: post-mortem CMR in Hypertrophic cardiomyopathy

Corresponding author:
Giovanni Donato Aquaro, M.D.
Fondazione Toscana G. Monasterio
Via Giuseppe Moruzzi, 1
56124 Pisa, Italy
Email: aquaro@ftgm.it
Phone: +39 - 050315 2818
Fax +39 – 050 315 2166
Twitter: @gdaqua

 doi:10.20944/preprints202011.0240.v1

ABSTRACT

Background: Post-mortem cardiac magnetic resonance (PMCMR) is an emerging tool supporting forensic medicine for the identification of the causes of cardiac death, as hypertrophic cardiomyopathy (HCM). We proposed a new method of PMCMR to diagnose HCM despite myocardial rigor mortis.

Methods: we performed CMR in 49 HCM patients, 30 non-HCM hypertrophy and 32 healthy controls. In cine images, rigor mortis was simulated by the analysis of the cardiac phase corresponding to the 25% of diastole. Left ventricular mass, mean and standard deviation (SD) of WT, maximal WT, minimal WT and their difference, were compared for the identification of HCM. These parameters were validated at PMCMR, evaluating 8 hearts with HCM, 10 with coronary artery disease and 10 with non-cardiac death.

Results: The SD of WT with a cut-off of > 2.4 had the highest accuracy to identify HCM (AUC 0.95, 95%CI 0.89-0.98). This was particularly evident in female population of HCM (AUC=0.998), with 100% specificity (95%CI 85-100%) and 96% sensitivity (95%CI 79-99%). Using this parameter, at PMCMR all the 8 patients with HCM were correctly identified with no false positive.

Conclusions: PMCMR allows to identify HCM as cause of sudden death using the SD of WT >2.4 as diagnostic parameter.

Keywords: Post-mortem Cardiac magnetic resonance; hypertrophic cardiomyopathy; sudden death

 doi:10.20944/preprints202011.0240.v1

Introduction

Hypertrophic cardiomyopathy is the most common cause of sudden death in young people, with particular predilection for children and young adults (1-3). Sudden death is frequently the first clinical manifestation of this disease, without warning signs or symptoms. Hypertrophic cardiomyopathy is the most frequent cause of sudden death in US competitive athletes (4). Despite sudden death is generally associated with vigorous physical exertion, most events are associated with mild exertion or even sedentary activities, including sleep.

HCM is characterized by extreme heterogeneity with regard to phenotypic expression, pathophysiology and clinical course. It is defined by the presence of increased left ventricular (LV) wall thickness, ranges from moderate (15 mm) to a massive (> 50 mm) hypertrophy in one or more left ventricular (LV) myocardial segments (1). The morphologic pattern of hypertrophy is either symmetrical or, more frequently, asymmetrical and in some cases HCM presents an unusual distribution as in the apical form.

 doi:10.20944/preprints202011.0240.v1

Histologic findings in patients with HCM reveal hypertrophied myocytes with nuclear pleomorphism and hyperchromasia, and myocardial disarray. However, myocyte disarray is not pathognomonic of HCM, and can be observed also in congenital heart diseases and in normal adult hearts, although usually mild and confined to the ventricular free wall-septal junctions.

Another common trait of HCM is the myocardial inclusions of areas of fibrosis in the myocardium. multiple post-mortem studies document gross macroscopic scarring in HCM patients who died suddenly, and the presence of myocardial interstitial fibrosis or fibrotic replacement at histopathological level. In addition small vessel arteries are structurally abnormal, and their lumen and vasodilatory capacity are decreased.

At present, autopsy and histological examination remain the gold standards for the post-mortem diagnosis of HCM, even if it is likely to be missed by pathologists at necropsy when the ipertrophy is mild and atypical distributed.

Cardiac magnetic resonance (CMR) is considered the gold standard imaging technique for the evaluation of cardiac morphology and function in hypertrophic cardiomyopathy (5). CMR allows evaluation of cardiac morphology, wall thickness and ventricular function permitting to diagnose HCM with great accuracy and reproducibility. CMR allows myocardial tissue characterization with the identification of myocardial edema and fibrosis providing prognostic stratification of patients with HCM (6).

In the last few years, post-mortem CMR (PMCMR) is being used as emerging technique for post-mortem radiological investigation of cardiovascular pathologies. PMCMR of explanted heart or of the entire body overcame limitations of spatial resolution permitting to acquire sub-millimetric high resolution images (7).

Using high resolution whole heart 3d-SSFP pulse sequence, PMCMR provide information of cardiac morphology with the identification of ventricular abnormalities associated with HCM (as coronary bridge, crypts, diverticuli, aneurysm, asymmetric or symmetric wall hypertrophy,

 doi:10.20944/preprints202011.0240.v1

papillary muscle abnormalities, valvular abnormalities, etc) and gives quantitative parameters as ventricular mass, volumes and atrial dimensions (7).

In HCM, LV mass could be normal, since a thickened wall is often associated to an opposite thinned one (8). For this reason, the assessment of the LV mass has shown a low discrimination strength to distinguish HCM from other cause of hypertrophy. Furthermore, the LV mass may be increased in other cardiac conditions as cardiac amyloidosis, aortic stenosis, Fabry disease and systemic hypertension.

In clinical setting the diagnosis of HCM is performed using the end-diastolic wall thickness of LV myocardium, but this is obviously not feasible at PMCMR because of the rigor mortis, that limits the diagnostic performance of PMCMR for this cardiomyopathy. Analogously to skeletal musculature, when ATP reserves of myocardium are consumed the heart remains in an early diastolic condition, called “rigor mortis”. The phase of cardiac cycle in which the heart becomes paralyzed during rigor mortis is highly variable. Indeed, a recent study by PMCMR, in patients with sudden cardiac death, showed that the ratio between LV myocardial volume and cavity volume in rigor mortis range from 2 to 43 demonstrating that rigor mortis may paralyze heart in both early and mid diastole without any relation with the time interval between death and PMCMR, sex, age and cardiac weight and body habitus (9).

In the present study we aimed to define new morphological parameters for the diagnosis of HCM in PMCMR, by simulating the rigor mortis in living patients with HCM (a), in patients with non-HCM hypertrophy (b), and in healthy controls (c), using the mid-diastolic cardiac phase of CMR cine images, and to test these parameters in PMCMR for the identification of HCM among patients with sudden death from other causes.

Preprints (www.preprints.org) | NOT PEER-REVIEWED | Posted: 6 November 2020 doi:10.20944/preprints202011.0240.v1

Methods

In-vivo study

We enrolled 50 patients with HCM and known pathogenic mutations of sarcomeric genes, 30 patients with LV hypertrophy of other causes (20 with cardiac amyloidosis, 10 with severe aortic stenosis) and 32 age and sex- healthy controls.

In vivo-CMR was performed using a 1.5T MRI scanner (General Electric Healthcare®, Milwaukee, Wisconsin) placed at the Fondazione Toscana Gabriele Monasterio, Pisa. A dedicated 16 channel cardiac coil.

A set of LV short axis cine images, acquired from the mitral plane valve to the LV ape were acquired using ECG triggered balanced steady-state free precession (bSSFP) pulse sequence with the following parameters: 30 phases, slice thickness 8 mm, no gap, views per segment 8, FOV 35-40 cm, phase FOV 1, matrix 224×224, reconstruction matrix 256×256, 45° flip angle, and a TR/TE near to 2 (10).

Analysis of bSSFP image were made using the MASS® Software Analysis (Leyden, The Netherlands). Briefly, using that software the end-systolic and the end-diastolic cardiac phase were visually identified as the cardiac phase having, respectively the lowest and the highest LV volume. Then, a mid-diastolic cardiac phase (25% of diastole) was chosen to simulate the rigor mortis state of post-mortem heart. In such cardiac phase, we measured LV wall thickness (WT) of all the conventional 17 myocardial segments using a semiautomatic approach. The LV endocardial and epicardial contour were manually traced with the exclusion of papillary muscles from LV mass. LV mass was measured as the myocardial LV volume multiplied for the myocardial density (1.05 g/cm3) (11). The average LV WT was measured for all the 17 segments. The following parameters

Preprints (www.preprints.org) | NOT PEER-REVIEWED | Posted: 6 November 2020 doi:10.20944/preprints202011.0240.v1

were evaluated: the average of LV WT, the SD of LV WT, maximal WT, the minimal WT, the difference between the maximal and minimal WT (max-minWT), and LV mass.

The presence of secondary features of HCM phenotype as LAD intramyocardial bridge, intramyocardial crypts and abnormalities of papillary muscles (number and morphology) were also evaluated.

The present study was approved by the local ethics committee and a written consent was obtained by all the enrolled patients (prot. n. 13896, approved on 25/10/2018).

Postmortem- Cardiac Magnetic Resonance

PMCMR was performed in 8 explanted heart of patients with sudden death and final histological and genetical diagnosis of HCM. PMCMR was also performed in 10 patients with sudden death and final diagnosis of coronary artery disease (CAD group) and in 10 patients with sudden death not caused by cardiac disease (non-cardiac death).

PMCMR was carried out with using the same 1.5T MRI scanner (General Electric Healthcare®, Milwaukee, Wisconsin) and 16-channel cardiac coil. A heart rate simulator with a set heart rate of 60 bpm was present. After the acquisition of triplane conventional localizer images, a 4-chamber localizer view was acquired using a single-shot SSFP sequence. Then, a whole-heart 3D-Fat Sat prepared SSFP pulse sequence was acquired with following parameters: slice thickness 0.9 mm, no gap, FOV 22x22 cm, phase FOV 1, matrix 256×256, reconstruction matrix 512×512, flip angle 45°, and a TR/TE ratio approximated to 2. From the 3D images a set of 2D SSFP LV short axis views from mitral valve plane to the apex were acquired with the following parameters: slice thickness 8 mm, no gap, FOV 35-40 cm, phase FOV 1, matrix 224×224, reconstruction matrix 256×256, 45° flip angle, and a TR/TE near to 2. Using the abovementioned MASS® software, the following parameters were calculated: the average of LV WT, the SD of LV WT, maximal WT, the minimal

 doi:10.20944/preprints202011.0240.v1

WT, the difference between the maximal and minimal WT (max-minWT), and LV mass. The presence of secondary features of HCM phenotype as LAD intramyocardial bridge, intramyocardial crypts and abnormalities of papillary muscles (number and morphology) were also evaluated.

Autopsy

According to the Guidelines for autopsy investigation of sudden cardiac death: 2017 update from the Association for European Cardiovascular Pathology, gross examination of the heart involved the evaluation of size and morphology, followed by the dissection of the organ trough multiple parallel slices from the apex to the mitral valve. The remainder of right and left ventricles in the basal half of the heart was dissected in the direction of flow of blood for eliciting the gross appearance of cardiac chambers and valves. Mid-cavity free wall thickness of the left and right ventricle and interventricular septum was measured. The transverse dimensions of both ventricles and atria were also measured.

Mapped labelled blocks from representative transverse slices of the ventricles were collected to include the apex, the free wall of the left ventricle (anterior, lateral, and posterior), the ventricular septum (anterior and posterior), and the free wall of the right ventricle (anterior, lateral, and posterior), as well as right ventricular outflow tract.

All samples were stained with Haematoxylin and Eosin (H&E). When necessary, immunohistochemistry or immunofluorescence for the characterization of inflammatory infiltrates, molecular screening and electron microscopy were performed.

Conventional autopsy included macroscopic, histologic and, when appropriate, further laboratory analyses as toxicology, chemistry, microbiology and genetic testing, that were performed according to national and international recommendations for forensic autopsy.

The final diagnosis was defined According to the cited Guidelines.

 doi:10.20944/preprints202011.0240.v1

2.4 Statistical analysis

Values are presented as the mean ± standard deviations (SD) or as the median (25^{th}-75^{th} percentiles) for variables with normal and non-normal distributions, respectively. Values with non-normal distribution according to Kolmogorov-Smirnov test were logarithmically transformed for parametric analysis. Qualitative data are expressed as percentages. Categorical variables were compared by the chi-squared test or the Fisher exact test when appropriate. Continuous variables were compared by the ANOVA t test and analysis of variance or by the Wilcoxon nonparametric test when appropriate. Bonferroni correction was used when needed. Receiver Operating Characteristic (ROC) curve analysis were used to test parameter for distinguish between HCM and other patients.

Results

In-vivo study

The final population of HCM included 49 patients (1 patient excluded for suboptimal image quality for atrial fibrillation), 24 males, mean age 53±12 years in HCM. The group of patients with other cause of LV hypertrophy (non-HCM Hypertrophy) included 30 patients, 18 males, with a mean age of 59±12 years. Finally, 32 healthy controls, with 15 males and mean age of 51±15 years.

In HCM groups 30(61%) patients had septal pattern of hypertrophy, 8 septal and apical hypertrophy (16%), 2 diffuse hypertrophy (4%), 1 with inferior-lateral hypertrophy (2%) and 8 with apical hypertrophy (16%) .

The SD of WT was significantly higher in HCM than in healthy controls (4.1±1.7 mm vs 1.4±0.4 mm, $p<0.001$), and in those with non-HCM hypertrophy (4.1±1.7 mm vs 2.1±0.7 mm, $p<0.001$).

 doi:10.20944/preprints202011.0240.v1

This difference was confirmed both in males (HCM vs healthy controls: 4.3±1.9 mm vs 1.5±0.4 mm, p<0.001; HCM vs non-HCM hypertrophy: 4.3±1.9 mm vs 2.3±0.7 mm, p<0.001) and females (HCM vs healthy controls: 3.8±1.3 mm vs 1.3±0.4 mm, p<0.001; HCM vs non-HCM hypertrophy: 3.8±1.3 mm vs 1.6±0.5 mm, p<0.001).

As shown in Table 1, HCM had also a significant higher maximal WT, minimal WT, mean WT, max-minD and left ventricular mass, compared to healthy controls. Compared to non-HCM hypertrophy, HCM had lower minimal WT, max-minD and LV mass.

Figures 3-6 showed the ROC curve analysis of LV mass, maximal WT, max-minD and SD of WT to distinguish between HCM and others.

As evident in the Figures and in table 2, at ROC curve analysis, the SD of WT with a cut-off of > 2.4 had the highest AUC (0.95, 95% CI 0.89-0.98) to distinguish between HCM and others in the whole population. The effectiveness of this parameter was particularly strong in females (AUC=0.998, 95% CI 0.92-1), showing a specificity of 100% (95% CI 85-100%) and a sensitivity of 96% (95% CI 79-99%).

PMCMR

PMCMR was performed in 8 patients with sudden cardiac death and HCM, 10 with sudden cardiac death and CAD, and 10 with non-cardiac death. In figure 7, it is showed an example of macroscopic and histological analysis in a case of HCM.

At PMCMR, in patients with confirmed HCM diagnosis the maximal WT was 24±6 mm, the SD of WT was 4.6 ± 1.9, the max-minD was 11 ± 5 mm. In patients with CAD, the maximal WT was 20±4 mm , the SD of WT was 2.1 ± 1.1, the max-minD was 6 ± 3 mm. In patients with non-cardiac death, the maximal WT was 19±3 mm, the SD of WT was 1.9 ± 0.8, the max-minD was 5 ± 2 mm.

 doi:10.20944/preprints202011.0240.v1

The maximal WT was not significantly different between HCM and CAD (p=0.10) but it was significantly higher in HCM than in non-cardiac death (p=0.03).

The max-minD was significantly higher in HCM than in CAD (p=0.005) and in non-cardiac death (p=0.0007). The SD of WT was significantly higher in HCM than in CAD (p=0.003) and in non-cardiac death (p=0.0009).

The cut-off of SD of WT found in the *in-vivo* study (>2.4) was able to detect all the 8 patients with HCM and none of the patients with CAD and with non-cardiac death. The maximal WT was >16 mm 7 out of 8 patients with HCM but also in 3 patients with CAD and in 4 with non-cardiac death. The max-minD was >9 mm in 6 out of 8 patients with HCM, in 2 with CAD and in none of non-cardiac death.

The SD of WT with 2.4 threshold had 100% sensitivity (95% CI 63-100) and 100% specificity (95% CI 83-100) to identify HCM. The maximal WT had 88%(95% CI 47-99) sensitivity and 68% (95%CI 45-86) specificity. Finally the max-minD 75%(95%CI 35-96) sensitivity and 91%(95% CI 70-98) specificity.

Discussion

In the present study we simulated in-vivo the rigor mortis of myocardium as the mid-diastolic phase of cardiac cycle (25% of diastole) and compared different parameters of LV morphology for the capability of detecting HCM from other cause of hypertrophy or healthy condition.

The LV mass, the mean WT, the SD of WT, the maximal and minimal WT and their difference.

 doi:10.20944/preprints202011.0240.v1

The main finding was that the SD of WT was the parameter with highest AUC to identify HCM. This parameter was particularly effective in female patients where demonstrated a 100% specificity and 96% sensitivity to identify HCM.

We tested all these parameters in explanted heart of patients dead for cardiac disease (HCM and CAD) and for non-cardiac death. The SD of WT was the unique parameter permitting to perfectly identify HCM from CAD and non-cardiac death.

These results are quite relevant because, demonstrated how it is possible to identify the HCM phenotype also in rigor mortis, highlighting the potentiality of PMCMR for the diagnosis of the cause of sudden cardiac death.

The morphological phenotype of HCM is heterogeneous. Sixteen different patterns of hypertrophy were described in HCM, but all of them are characterized by asymmetrical hypertrophy (12). Hypertrophy in HCM is most frequently located in the interventricular septum, but it may be also found in both septum and apical region, or it may be limited to apical segments or to the inferolateral segments (13). Yet, in a not negligible percentage of cases hypertrophy has a diffuse pattern of distribution, involving the majority of myocardial segments, but also in these situations the WT are heterogeneous.

The SD of WT is, indeed, a measure of this heterogenous distribution of WT in HCM and then, the results of the current study are not surprising.

This new parameter of PMCMR may help to diagnose HCM as cause of sudden cardiac death. In HCM histologic findings reveal hypertrophied myocytes with nuclear pleomorphism and hyperchromasia, and myocardial disarray (14.). However, myocyte disarray is not pathognomonic of HCM, and can be observed also in congenital heart diseases and in normal adult hearts, although usually mild and confined to the ventricular free wall-septal junctions. Only when assessed

Preprints (www.preprints.org) | NOT PEER-REVIEWED | Posted: 6 November 2020 doi:10.20944/preprints202011.0240.v1

quantitatively of > 10% hearth, disarray is considered diagnostic of HCM. The diagnostic significance of a lower percentage of myocyte disarray has not been determined yet (15).

Another hallmark of HCM is the myocardial inclusions of areas of fibrosis in the myocardium. Furthermore, multiple post-mortem studies document an abnormal structure of intramural small vessel with different grade of lumen stenosis (16). It has been hypothesized that the fibrotic replacement secondary to ischemia and the myocardial scars represent a potentially arrhythmogenic substrate increasing the patient's susceptibility to ventricular tachycardia/fibrillation and the risk of sudden death. In the asymmetrical septal variant of HCM, the gross examination may reveal the thickening of the basal anterior septum with subaortic bulging leading to left ventricular outflow tract obstruction. Septal endocardial friction lesions associated to this finding are also observed. However, the final diagnosis of HCM implies exclusion of abnormal loading conditions which leads to a secondary ventricular hypertrophy and other diseases that mimic HCM, including cardiac amyloidosis, Fabry disease, glycogen storage disease and mitochondrial cardiomyopathies. An exercise-induced hypertrophy has also to be differentiated (17).

It is worth of note that the SD of WT was particularly able to identify females with HCM. HCM females had worse prognosis than males (18). The diagnostic cut-off of ≥15 mm of end-diastolic WT, which widely accepted as diagnostic criterion for HCM, is the valid for both sexes. However, considering the lower body weight and height, this cut-off could be too high for female patients and be associated with a more advanced stage of disease. In females the SD of WT could be useful to detect HCM in earlier stages when the maximal end-diastolic WT is yet <15 mm. Future studies are needed to test this hypothesis.

Limitations

Some study limitations should be mentioned. First, in the in-vivo study, we simulated rigor mortis as the phase of cardiac cycle corresponding to the 25% of diastole. This may be an over-

 doi:10.20944/preprints202011.0240.v1

simplification, because as demonstrated by Bonzon et al (9), the rigor mortis may paralyse heart indifferently in any phase of early and mid diastole. The WT and derived parameters could change in different diastolic phases. However, we the results of the PMCMR study in explanted heart confirmed the effectiveness of our method to distinguish between HCM and other cause of death and overcome this limitation.

Second, the PMCMR study included only HCM and CAD of cause of sudden death, and non-cardiac death. Future studies are needed to evaluate the effectiveness of SD of WT to detecting HCM when compared to other cause of cardiac death.

Conclusions

Among the different morphological parameters, the SD of WT is the most accurate to identify HCM during rigor mortis. This parameters was tested in a cohort of patients by simulation of rigor mortis, through the analysis of cine images of mid-diastolic phase of cardiac cycle, and validated in explanted heart by PMCMR. The SD of WT >2.4 is effective in all the population with HCM but it is particularly accurate in female population. Further studies are needed to evaluate its effectiveness in real-life forensic medicine.

Patents:

not reported

References:

1. Maron BJ, Maron MS. Hypertrophic cardiomyopathy. Lancet 2013;381:242-255.

2. Elliott PM, Poloniecki J, Dickie S, Sharma S, Monserrat L, Varnava A, Mahon NG, McKenna WJ. Sudden death in hypertrophic cardiomyopathy: identification of high risk patients. J Am Coll Cardiol. 2000;36:2212– 2218.

3. Maron BJ. Contemporary insights and strategies for risk stratification and prevention of sudden death in hypertrophic cardiomyopathy. Circulation 2010; 121: 445–56.

4. Maron BJ, Doerer JJ, Haas TS, Tierney DM, Mueller FO. Sudden deaths in young competitive athletes: analysis of 1866 deaths in the United States, 1980–2006. Circulation 2009; 119: 1085–92.

5. Quarta G, Aquaro GD, Pedrotti P, Pontone G, Dellegrottaglie S, Iacovoni A, Brambilla P, Pradella S, Todiere G, Rigo F, Bucciarelli-Ducci C, Limongelli G, Roghi A, Olivotto I.Cardiovascular magnetic resonance imaging in hypertrophic cardiomyopathy: the importance of clinical context.Eur Heart J Cardiovasc Imaging. 2018 Jun 1;19(6):601-610

6. Todiere G, Pisciella L, Barison A, Del Franco A, Zachara E, Piaggi P, Re F, Pingitore A, Emdin M, Lombardi M, Aquaro GD.Abnormal T2-STIR magnetic resonance in hypertrophic cardiomyopathy: a marker of advanced disease and electrical myocardial instability. PLoS One. 2014;9:e111366

7. Guidi B, **Aquaro GD**, Gesi M, Emdin M, Di Paolo M.Postmortem cardiac magnetic resonance in sudden cardiac death. Heart Fail Rev. 2018;23:651-665

8. Olivotto I, Maron MS, Autore C, Lesser JR, Rega L, Casolo G, De Santis M, Quarta G, Nistri S, Cecchi F, Salton CJ, Udelson JE, Manning WJ, Maron BJ. Assessment and

significance of left ventricular mass by cardiovascular magnetic resonance in hypertrophic cardiomyopathy. J Am Coll Cardiol. 2008;52:559-66

9. Bonzon J, Schön CA, Schwendener N, Zech WD, Kara L, Persson A, Jackowski C. Rigor mortis at the myocardium investigated by post-mortem magnetic resonance imaging. Forensic Sci Int. 2015 Dec;257:93-97
10. Lionetti V, Aquaro G,Simioniuc A,Di Cristofano C,Forini F,Cecchetti F,Campan M,De Marchi D,Bernini F,Grana M,Nannipieri M,Mancini M,Lombardi M,Recchia F,Pingitore A. Severe Mechanical Dyssynchrony Causes Regional Hibernation-Like Changes in Pigs With Nonischemic Heart Failure.Journal of Cardiac Failure 2009;15:920-928
11. Aquaro GD, Ait-Ali L, Basso ML, Lombardi M, Pingitore A, Festa P.Elastic properties of aortic wall in patients with bicuspid aortic valve by magnetic resonance imaging. Am J Cardiol. 2011;108:81-87
12. Klues HG, Schiffers A, Maron BJ. Phenotypic spectrum and patterns of left ventricular hypertrophy in hypertrophic cardiomyopathy: morphologic observations and significance as assessed by two-dimensional echocardiography in 600 patients. J Am Coll Cardiol 1995;26:1699–708
13. (Florian A, Masci PG, De Buck S, Aquaro GD, Claus P, Todiere G, Van Cleemput J, Lombardi M, Bogaert J. Geometric assessment of asymmetric septal hypertrophic cardiomyopathy by CMR. JACC Cardiovasc Imaging. 2012;5:702-11

14. Amanda M. Varnava, Perry M. Elliott, Christina Baboonian, Fergus Davison, Michael J. Davies, and William J. McKenna. Hypertrophic cardiomyopathy: histopathological features of sudden death in cardiac troponin t disease. Circulation, 104(12):1380–1384, 2001

15. Hata Y, Ichimata S, Yamaguchi Y, et al. Clinicopathological and Genetic Profiles of Cases with Myocytes Disarray-Investigation for Establishing the Autopsy Diagnostic Criteria for Hypertrophic Cardiomyopathy. J Clin Med. 2019;8(4):463

16. Basso C, Thiene G, Corrado D, et al. Hypertrophic cardiomyopathy and sudden death in the young: pathologic evidence of myocardial ischemia.Hum Pathol. 2000;31:988–998

17. (Elliott PM, Anastasakis A, Borger MA, et al. 2014 ESC Guidelines on diagnosis and management of hypertrophic cardiomyopathy: the Task Force for the Diagnosis and Management of Hypertrophic Cardiomyopathy of the European Society of Cardiology (ESC). Eur Heart J. 2014;35:2733–2779

18. Todiere G, Nugara C, Gentile G, Negri F, Bianco F, Falletta C, Novo G, Di Bella G, De Caterina R, Zachara E, Re F, Clemenza F, Sinagra G, Emdin M, Aquaro GD. Prognostic Role of Late Gadolinium Enhancement in Patients With Hypertrophic Cardiomyopathy and Low-to-Intermediate Sudden Cardiac Death Risk Score. Am J Cardiol 2019;124:1286-1292

Figure legends:

Figure 1: Example of in-vivo analysis of cine-SSFP images. The cardiac phase corresponding to the 25% of diastole was chosen to simulate rigor mortis. Endocardial and epicardial contours were manually traced excluding papillary muscles. The average myocardial wall thickness (WT) was automatically measured in each of the 17 conventional myocardial segments. The left ventricular

 doi:10.20944/preprints202011.0240.v1

(LV) mass, the mean WT, the standard deviation (SD) of WT, the maximal WT, the minimal WT and the maximal-minimal difference of WT were measured.

Figure 2: example of analysis of post-mortem cardiac magnetic resonance image. In this images, the endocardial and epicardial contours were traced and the myocardial thickness of all the 17 myocardial segments was measured. The same parameters of figure 1 were obtained

Figure 3: Receiver Operating Characteristic curves of the LV mass for the identification of patients with HCM in the whole population.

Figure 4: Receiver Operating Characteristic curves of the Maximal wall thickenss (WT) for the identification of patients with HCM in the whole population, in males and females.

Figure 5: Receiver Operating Characteristic curves of the difference between maximal and minimal wall thickness (WT) for the identification of patients with HCM in the whole population, in males and females.

Figure 6: Receiver Operating Characteristic curves of the standard deviation of wall thickness (WT) for the identification of patients with HCM in the whole population, in males and females.

Figure 7: pathology findings in a case of a HCM patient of 22 years old with sudden death. Gross examination 270 gr - 1° In section, mild left ventricular hypertrophy and mild papillary muscle hypertrophy (A and B) Histological evaluation of the LV free wall showing cardiomyocyte enlargement and disarray (C, hematoxylin-eosin staining, 200×) and interfascicular fibrosis (D, Masson's trichrome staining, 200×).

 doi:10.20944/preprints202011.0240.v1

 doi:10.20944/preprints202011.0240.v1

	Healthy controls	P value[1]	HCM	p value[2]	Non-HCM hypertrophy
n.	32		49		30
Age (years)	48 ± 15	0.3	53 ± 12	<0.001	69 ± 12
Males, n (%)	15 (47%)	0.7	24 (50%)	0.15	18 (60%)
Maximal WT whole population (mm)	11 ± 2	<0.001	21 ± 5	0.07	19 ± 4
Maximal WT males (mm)	12 ± 1	<0.001	22 ± 5	0.17	20 ± 4
Maximal WT females (mm)	11 ± 2	<0.001	20 ± 5	0.07	16 ± 3
Minimal WT whole population (mm)	6 ± 1	0.004	7 ± 2	<0.001	11 ± 3
Minimal WT males (mm)	7 ± 1	0.14	8 ± 2	<0.001	12 ± 2
Minimal WT females (mm)	6 ± 1	0.007	7 ± 2	<0.001	11 ± 4
Mean WT whole population (mm)	8 ± 1	<0.001	14 ± 3	0.053	15 ± 3
Mean WT males (mm)	9 ± 1	<0.001	14 ± 3	0.07	16 ± 3
Mean WT females (mm)	8 ± 1	<0.001	13 ± 3	0.95	13 ± 3
Max-minD whole population (mm)	5 ± 1	<0.001	14 ± 5	<0.001	8 ± 3
Max-minD males (mm)	5 ± 2	<0.001	15 ± 6	<0.001	9 ± 3
Max-minD females (mm)	5 ± 1	<0.001	13 ± 5	<0.001	6 ± 2
LV mass whole population (g)	102 ± 25	<0.001	160 ± 54	0.03	193 ± 60
LV mass males (g)	118 ± 17	<0.001	178 ± 52	0.012	221 ± 43
LV mass females (g)	85 ± 19	<0.001	141 ± 50	0.5	126 ± 34
SD of WT, whole population	1.4 ± 0.4	<0.001	4.1 ± 1.7	<0.001	2.1 ± 0.7
SD of WT, males	1.5 ± 0.4	<0.001	4.3 ± 2.0	<0.001	2.3 ± 0.7
SD of WT, females	1.3 ± 0.4	<0.001	3.8 ± 1.3	<0.001	1.6 ± 0.5

Table 1. Comparison of morphometric features between different groups.

HCM, hypertrophy cardiomyopathy; Non-HCM hypertrophy included 20 patients with cardiac amyloidosis and 10 with aortic stenosis.

[1], p value of healthy controls vs HCM comparison; [2], p value of HCM vs non-HCM hypertrophy comparison.

WT, wall thickness; Max-MinD, difference between the maximal and mimal wall thickness; SD, standard deviation.

 doi:10.20944/preprints202011.0240.v1

 doi:10.20944/preprints202011.0240.v1

Table 2: results of ROC curve analysis for distinguish between HCM and others

Parameters:	Cut-off	Specificity	Sensitivity	AUC	p value	Standard error
Whole population						
LV mass	>122g	58 (43-72)	77 (63-88)	0.64 (0.54-0.73)	0.016	0.06
Maximal WT	≥16mm	71 (57-83)	96 (86-99)	0.85(0.77-0.92)	<0.0001	0.04
Minimal WT	≤11mm	19 (10-33)	100 (93-100)	0.54 (0.43-0.64)	0.53	0.06
Mean WT	>11mm	62 (47-75)	92 (80-98)	0.73 (0.63-0.81)	<0.0001	0.05
Max-minD	>9mm	88 (77-96)	86 (73-54)	0.94 (0.88-0.98)	<0.0001	0.02
SD of WT	>2.4	85 (72-93)	90 (78-97)	0.95 (0.89-0.98)	<0.0001	0.02
Males						
LV mass	>130g	41 (24-61)	84 (64-96)	0.56 (0.42-0.70)	0.44	0.08
Maximal WT	>16mm	55 (36-74)	100 (86-100)	0.82 (0.69-0.91)	<0.0001	0.06
Minimal WT	≤11mm	31 (15-51)	100 (86-100)	0.61 (0.47-0.74)	0.14	0.08
Mean WT	>11mm	52 (33-71)	96 (80-99)	0.65 (0.51-0.74)	0.05	0.08
Max-minD	>10mm	89 (73-98)	84 (64-96)	0.91 (0.79-0.97)	<0.0001	0.04
SD of WT	>2.6	86 (68-96)	84 (64-96)	0.91 (0.80-0.97)	<0.0001	0.04
Females						
LV mass	>122g	90 (70-99)	65 (43-84)	0.79 (0.64-0.89)	0.0001	0.07
Maximal WT	>16mm	91 (72-98)	92 (73-99)	0.93 (0.81-0.98)	<0.0001	0.04
Minimal WT	>7mm	56 (35-77)	67 (44-84)	0.59 (0.44-0.73)	0.28	0.09
Mean WT	>11mm	83 (61-95)	88 (68-97)	0.86 (0.73-0.95)	<0.0001	0.06
Max-minD	>7mm	96 (78-99	96 (79-99)	0.993 (0.91-1)	<0.0001	0.008
SD of WT	>2.3	100 (85-100)	96 (79-99)	0.998 (0.92-1)	<0.0001	0.003

WT, wall thickness; Max-MinD, difference between the maximal and mimal wall thickness; SD, standard deviation.

 doi:10.20944/preprints202011.0240.v1

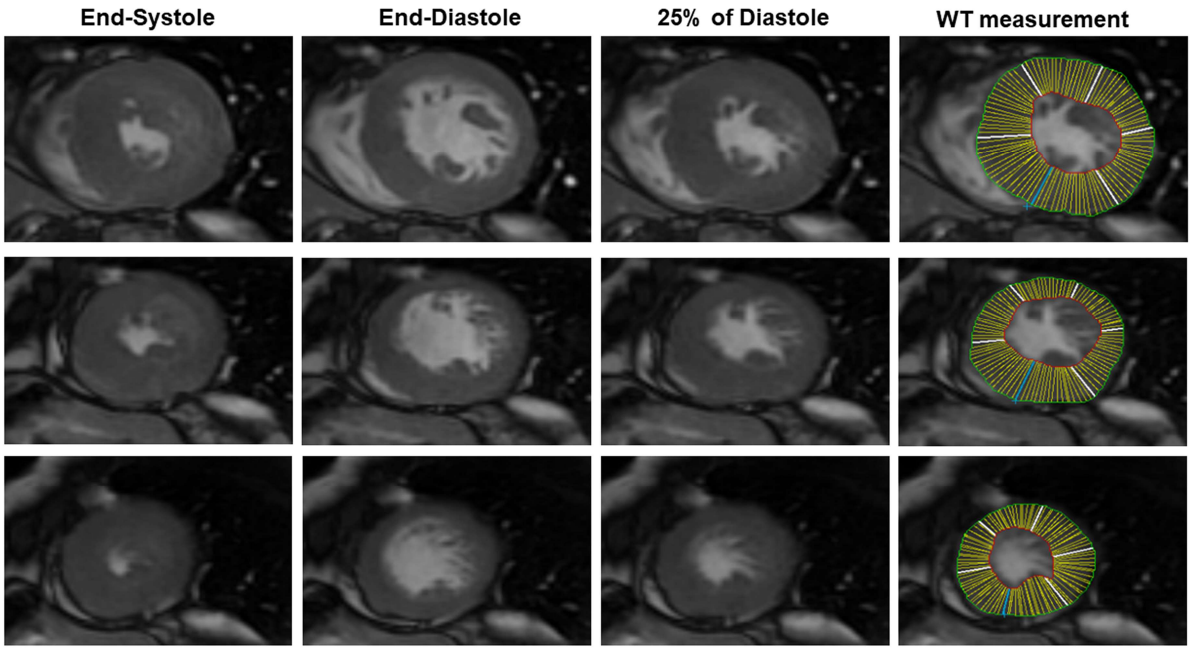

 doi:10.20944/preprints202011.0240.v1

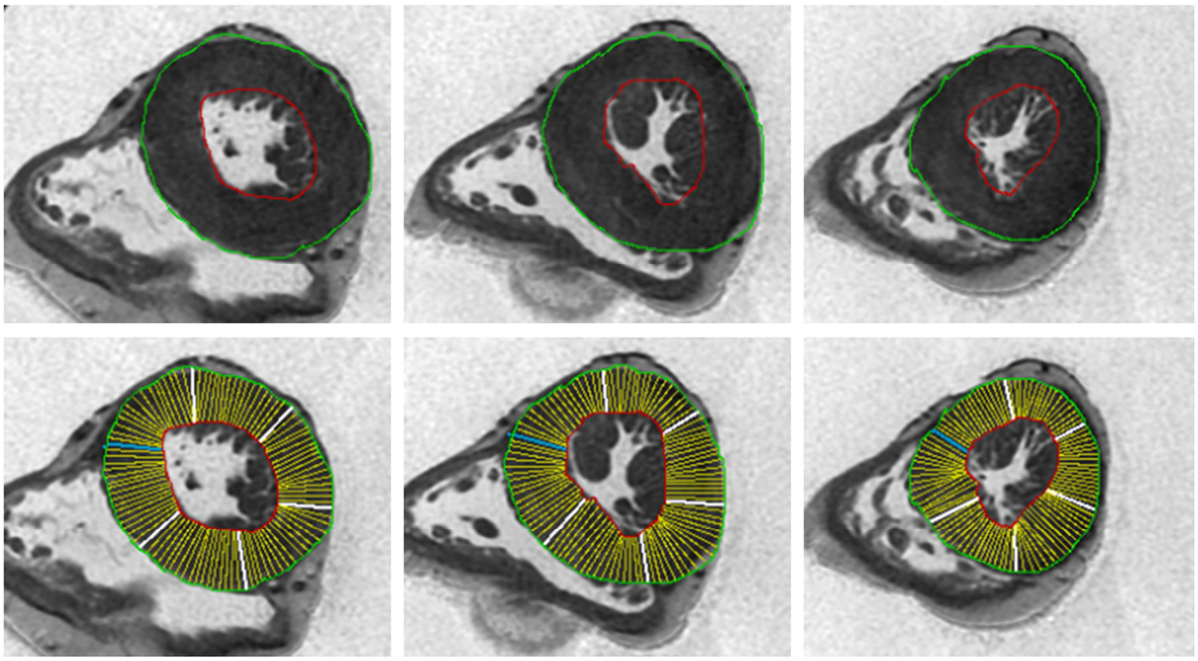

Preprints (www.preprints.org) | NOT PEER-REVIEWED | Posted: 6 November 2020 doi:10.20944/preprints202011.0240.v1

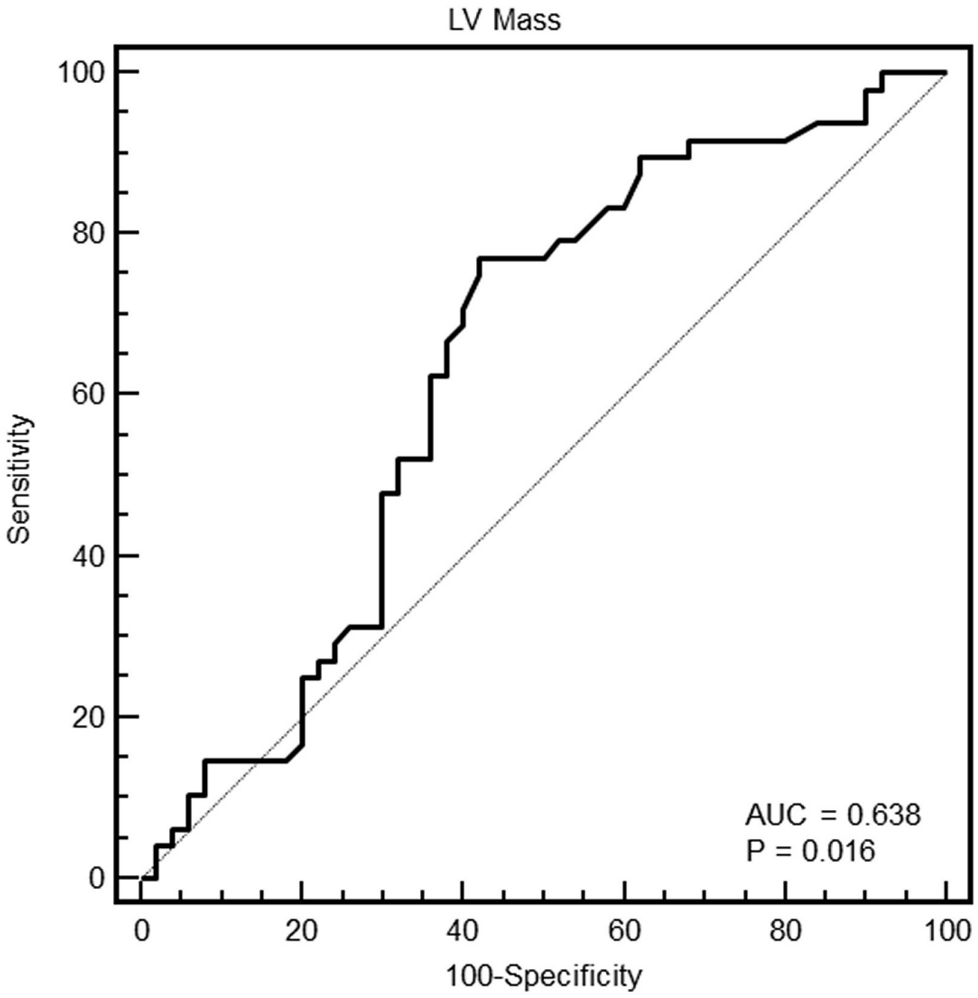

Preprints (www.preprints.org) | NOT PEER-REVIEWED | Posted: 6 November 2020 doi:10.20944/preprints202011.0240.v1

Figure 4

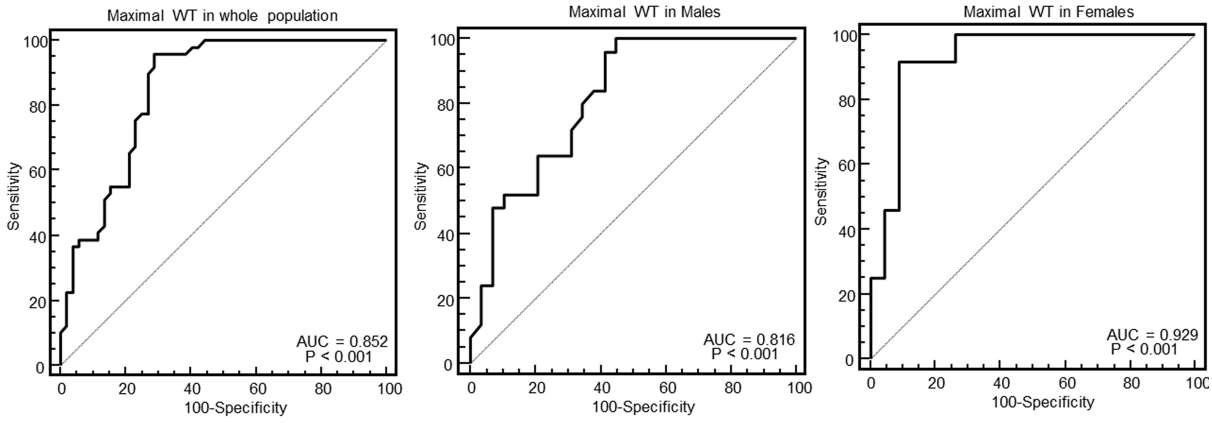

Preprints (www.preprints.org) | NOT PEER-REVIEWED | Posted: 6 November 2020 doi:10.20944/preprints202011.0240.v1

Figure 5

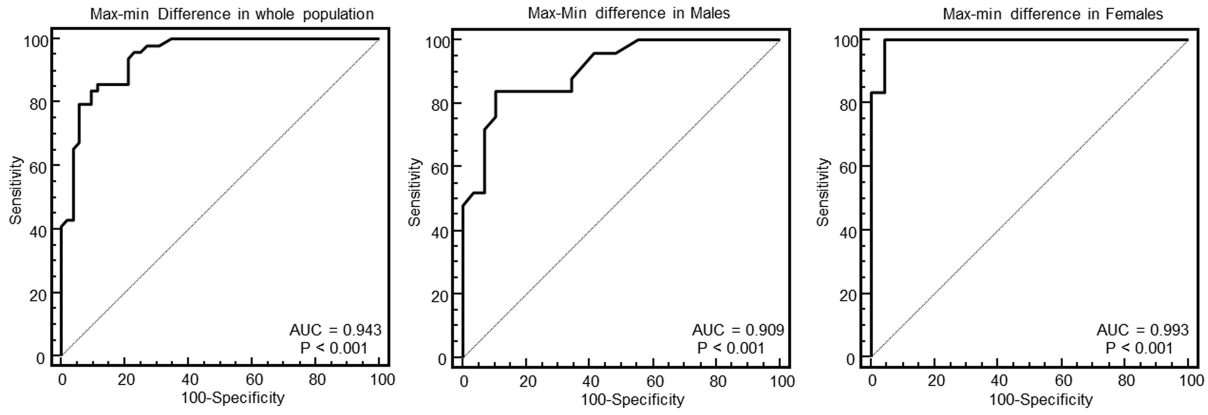

Preprints (www.preprints.org) | NOT PEER-REVIEWED | Posted: 6 November 2020 doi:10.20944/preprints202011.0240.v1

Figure 6

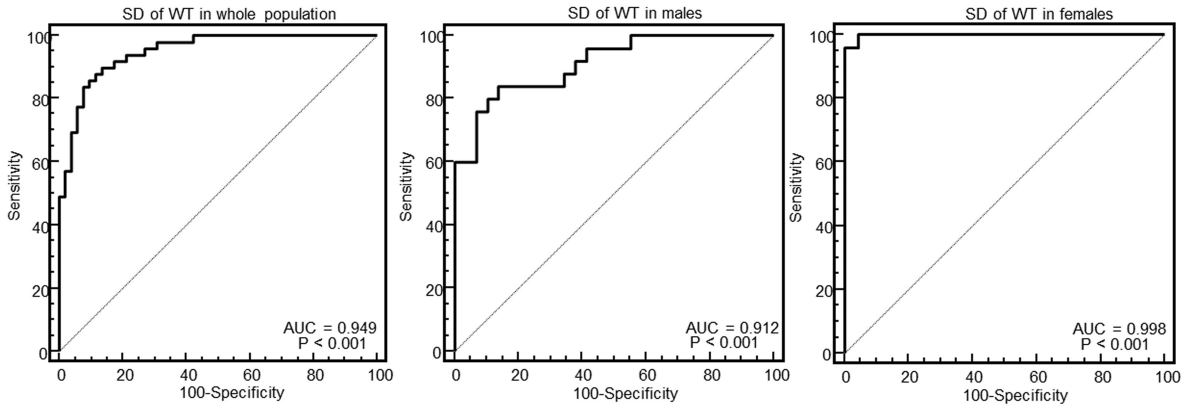

Preprints (www.preprints.org) | NOT PEER-REVIEWED | Posted: 6 November 2020 doi:10.20944/preprints202011.0240.v1

Figure 7